Clustering of topological defects in two-dimensional melting of active and passive disks

Pasquale Digregorio,[1] Demian Levis,[2,3] Leticia F. Cugliandolo,[4,5] Giuseppe Gonnella,[1] and Ignacio Pagonabarraga[2,3]

[1] *Dipartimento di Fisica, Università degli Studi di Bari and INFN, Sezione di Bari, via Amendola 173, Bari, I-70126, Italy*
[2] *CECAM Centre Européen de Calcul Atomique et Moléculaire, Ecole Polytechnique Fédérale de Lausanne, Batochimie, Avenue Forel 2, 1015 Lausanne, Switzerland*
[3] *UBICS University of Barcelona Institute of Complex Systems, Martí i Franquès 1, E08028 Barcelona, Spain*
[4] *Sorbonne Université, Laboratoire de Physique Théorique et Hautes Energies, CNRS UMR 7589, 4 Place Jussieu, 75252 Paris Cedex 05, France*
[5] *Institut Universitaire de France, 1 rue Descartes, 75005 Paris France*

(Dated: November 18, 2019)

We provide a quantitative analysis of all kinds of topological defects present in 2D passive and active repulsive disk systems. We show that the passage from the solid to the hexatic is driven by the unbinding of dislocations. Instead, although we see dissociation of disclinations as soon as the liquid phase appears, extended clusters of defects largely dominate below the solid-hexatic critical line. The latter percolate at the hexatic-liquid transition in continuous cases or within the coexistence region in discontinuous ones, and their form gets more ramified for increasing activity.

arXiv:1911.06366v1 [cond-mat.soft] 14 Nov 2019

In two-dimensions (2D), thermal fluctuations often prevent the emergence of long-range order (LRO), as illustrated by the absence of spontaneous magnetization in 2D Heisenberg magnets [1] and positional order in 2D particle systems [2]. However, different kinds of phase transitions driven by topological defects can still occur: for example, in 2D planar magnets, the binding-unbinding of vortices mediate the so-called Berezenskii-Kosterlitz-Thouless (BKT) transition between a paramagnet and a low temperature critical phase with quasi-long-range magnetic order (QLRO) [3, 4].

The nature of the melting transition in 2D crystals is far more involved and controversial [5, 6], partly due to the fact that particle systems might have two types of order, translational and orientational, and thus two kinds of topological defects, dislocations and disclinations. The most standard picture of 2D melting in spherically symmetric particle systems follows the work of Kosterlitz-Thouless-Halperin-Nelson-Young (KTHNY) [7, 8], according to which the transition from the solid (with positional QLRO and orientational LRO) to the isotropic liquid occurs in two-steps, separated by an intermediate hexatic phase characterized by orientational QLRO. These solid-hexatic and hexatic-liquid transitions are of BKT type, driven by the unbinding of dislocations and disclinations, respectively. While evidence for the KTHNY scenario has been given in some experiments [9] and simulations [10–13], alternative mechanisms have also been proposed [5, 6] and, in particular, one in which the continuous two-step scenario is preempted by a single solid-liquid first-order transition driven by the aggregation of defects into grain-boundary-like structures [14–16]. Recent simulations [17–19] and experiments [20] have shown that the melting of equilibrium (passive) repulsive disks shares aspects of both scenarios: a BKT solid-hexatic transition but a first-order hexatic-liquid one, if the interaction potential is stiff enough. It has thus been suggested that the disclination-unbinding mechanism should be preempted by a first-order transition involving the proliferation of clusters of defects, forming a percolating network in the liquid regime [12, 18, 19]. However, neither a quantitative analysis of such clusters nor the derivation of a theory for the stability of the hexatic phase against grain-boundaries have been conducted. Moreover, and surprisingly enough, no clear experimental evidence and very little numerical one [19] for dislocation unbinding at the solid-hexatic transition exists.

Besides the issues that still remain unclear for systems of passive particles, the classical problem of 2D phase transitions is experiencing a resurge of interest in the context of active matter systems. These are collections of self-propelled particles which pump energy from their environment and convert it into motion in the presence of dissipation, but in a way that breaks detailed balance [21–23]. The question now is how these non-equilibrium 'active' fluctuations affect the phase behavior of 2D particle systems [24–28] and the role played by topological defects. It has recently been shown that self-propelled hard-disks follow the two-step melting scenario of their passive counterparts at small activities, up to a threshold above which hexatic-liquid coexistence, characteristic of the first-order nature of the transition, disappears [26, 28]. Both the hexatic-liquid and solid-hexatic transitions are shifted to higher densities as the degree of activity is increased and, at sufficiently high activities, these transitions overlap with a coexistence region purely triggered by self-propulsion, the so-called Motility-Induced Phase-Separation (MIPS) [29]. Although topological defects are known to be crucial in understanding 2D equilibrium phase transitions, little attention has been paid to their study in self-propelled systems [25, 28] and thus the very nature of the phase transitions is still to be understood.

In this Letter we systematically study the full spectrum

of topological defects in 2D systems of passive hard and soft, and active hard disks. Besides a careful analysis of point-like defects, we also characterize more complex structures, in the form of extended clusters. We first show that the solid-hexatic transition is driven by the unbinding of dislocations and agrees with the KTHNY scenario at all activities. Next, we find that 2D melting is generically accompanied by cluster *percolation* close to the hexatic-liquid transition, both for active and passive systems. Although the presence of a spanning cluster, similar to critical percolation, seems to be independent of the order of the transition, the nature and geometry of the clusters does vary from case to case.

We consider N Active Brownian Particles (ABP) located at $\mathbf{r}_i$ in an $L_x \times L_y$ box with periodic boundary conditions and obeying (see [26] for details)

$$\begin{aligned} \gamma\dot{\mathbf{r}}_i &= F_{\rm act}\mathbf{n}_i - \textstyle\sum_{j(\neq i)} \boldsymbol{\nabla}_i U(r_{ij}) + \sqrt{2\gamma k_B T}\boldsymbol{\xi}_i \,, \\ \dot{\theta}_i &= \sqrt{2D_\theta}\eta_i \,, \end{aligned} \tag{1}$$

where $F_{\rm act}$ is the self-propulsion force acting along $\mathbf{n}_i = (\cos\theta_i(t), \sin\theta_i(t))$, $r_{ij} = |\mathbf{r}_i - \mathbf{r}_j|$ and $U(r)$ is a repulsive (i) hardcore $U^H(r) = 4\varepsilon[(\sigma/r)^{64} - (\sigma/r)^{32}] + \varepsilon$ if $r < \sigma_d = 2^{1/32}\sigma$ and 0 otherwise or (ii) soft $U^S(r) = \varepsilon(\sigma_d/r)^6$ if $r < 2.6\ \sigma_d$ potential [18]. The components of $\boldsymbol{\xi}$ and η are zero-mean and unit variance independent white Gaussian noises. The units of length and energy are given by σ_d and ε, respectively. We fix $D_\theta = 3k_BT/\sigma_d^2\gamma$, $\gamma = 10$, $N = 512^2$, and $k_BT = 0.05$ for the hard disks and $k_BT = 1$ for the soft ones. We vary the packing fraction $\phi = \pi\sigma_d^2 N/(4L_xL_y)$, where $L_x/L_y = 2/\sqrt{3}$, and the Péclet number $\mathrm{Pe} = F_{\rm act}\sigma_d/(k_BT)$.

The topological defects are mis-coordinated particles, or cells in the Voronoi construction, with respect to the hexagonal lattice. Free disclinations correspond to individual cells with 5 or 7 neighbors (5-fold and 7-fold defects), while free dislocations to pairs of neighboring cells with 5 and 7 neighbors (5-7 pairs). Vacancies, point defects resulting from the removal of a particle in an hexagonal packing, can be identified with different configurations involving, either groups of pairs of bounded dislocations (two or more), or higher order mis-coordinated cells (with less than 5 or more than 7 neighbours), see Fig. 1. The number density of each kind of defect is defined as the ratio between the number of cells with the selected type of defect and the total number of cells. The free disclination, free dislocation, vacancy and cluster values are shown in Fig. 2 in four representative cases: (i) passive hard-disks, Pe = 0; (ii) passive soft-disks, Pe = 0; (iii) ABP at Pe = 20 (for which the liquid-hexatic transition is continuous); (iv) ABP at Pe = 100 (which exhibits MIPS) [26]. In the MIPS coexistence region, we only count defects belonging to the dense phase.

The first noticeable fact in all panels concerns the transition between the solid and hexatic phases. Free disclinations and dislocations are absent in the solid phase (orange) of hard systems (a), (c) and (d). At the vicinity of the hexatic phase (blue), the number of free dislocations increases sharply, indicating that they break positional QLRO and mediate the solid-hexatic transition for all Pe. For soft particles this number is different from zero at all ϕ but its variation is faster below the transition (b). Such behavior departs from a recent study reporting that the melting of the active solid is not driven by the proliferation of dislocations, as a KTHNY scenario would predict, opening the possibility of breaking orientational LRO in the absence of any defect [28].

As regards free disclinations, their density is very close to zero in the hexatic and detaches significantly from this value when the liquid appears, either as a pure phase (b) and (c) or co-existing with the hexatic (a) and (d). The KTHNY unbinding arises in the liquid component.

The density of each kind of defect (inset Fig. 2 (d)) remains almost unchanged below the point where orientational correlations change behavior from algebraic to exponential (blue dashed line, see [26]) in the MIPS coexistence region and until the low density spinodal [26, 30]. This means that the dense phase generated through MIPS is characterized by a given number of defects set by Pe and not ϕ. (For more details on the behavior beyond the dashed line and spinodal see the SM [31].)

Importantly enough, most mis-coordinated cells cannot be identified as disclinations or dislocations, but appear in clusters comprising defects of alternating topological charge. These objects lie beyond the KTHNY theory (see Fig. 1) and, to understand the role they play, we systematically analyze them. Vacancies do not break

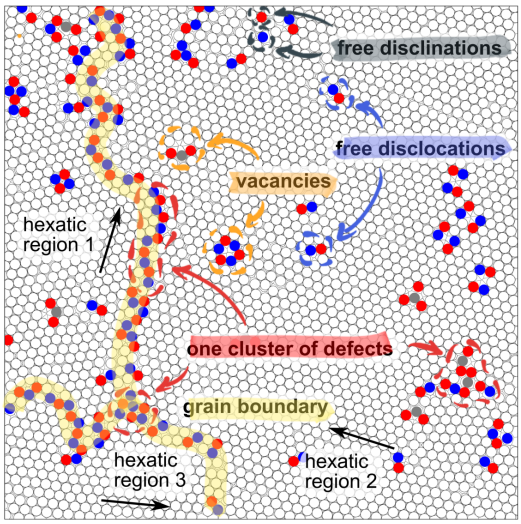

FIG. 1. (Color online.) Detailed view of a typical snapshot (Pe = 20 and $\phi = 0.820$) with different kinds of defects. Particles in 5-fold cells are colored in red, 7-fold ones in blue, and all other mis-coordinated ones in grey. Disclinations are highlighted in grey, dislocations in blue, vacancies in orange and clusters of defects in red. A grain boundary delimiting regions with different hexatic order is marked in yellow.

positional QLRO and can thus be present in the solid phase. As shown in Fig. 2 (d), at high Pe (e.g. Pe = 100) the number of vacancies increases as we decrease ϕ in the solid regime and rapidly decays as we get into the hexatic, with a peak at the transition. Such decay is concomitant with an increase in the number of free dislocations: vacancies leave away free dislocations. Vacancies must be distinguished from defect clusters that do break positional order. To do so, we associate a unit vector e_{ij} to each pair of neighboring defects, pointing from a cell with coordination number $m_i < 6$ to a neighboring one with $m_j > 6$ (see Fig. 1). If the sum of these vectors over all the cells in a structure of more than 2 connected mis-coordinated cells, is smaller than half the mean distance between particles, we identify it as a vacancy, and as a cluster otherwise [32]. (In this counting, a bounded dislocation pair is equivalent to a vacancy.)

As shown in Fig. 2, clusters dominate the distribution of defects in the hexatic phase, proving that topological excitations are collective rather than localized in this regime. Importantly, this also suggests that their proliferation might drive melting, instead of the unbinding of disclinations. Clusters of defects in hard-disk systems have been associated to the formation of grain boundaries delimiting regions of different hexatic order [18, 19], which could drive an alternative first-order melting mechanism in 2D [14–16]. However, the relationship between generic clusters of defects as counted here, and grain boundaries, is not clear yet. Moreover, for passive soft-disks and active hard-disks at Pe = 20, there is no evidence for a first-order transition, and yet the density of clusters at the liquid-hexatic transition is very close to the passive hard-disk value (≈ 0.05). This suggests, as we show below, that the proliferation of clusters might be generic and not responsible for the first-order character of the hexatic-liquid transition of passive hard-disks.

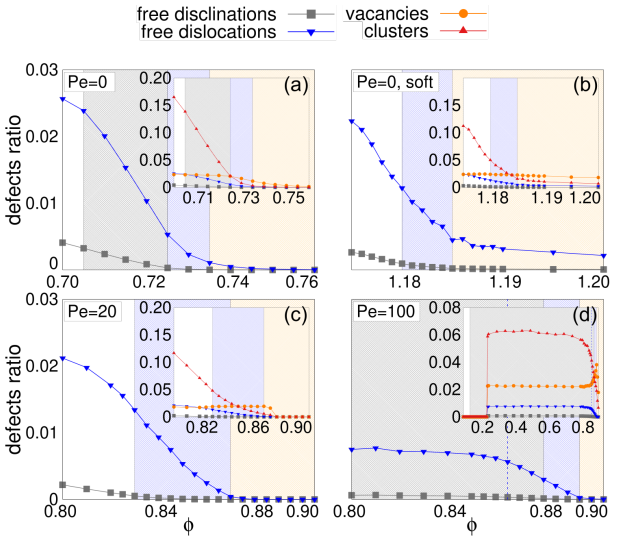

FIG. 2. (Color online.) Normalized number of dislocations and disclinations as a function of ϕ for passive hard-disks (a), passive soft-disks (b), ABP at Pe = 20 (c) and Pe = 100 (d). All defects, including vacancies and clusters of defects, are shown in the insets. The solid, hexatic, phase-coexistence and liquid regions are shown in orange, blue, grey and white, respectively. The dashed blue line inside the MIPS region (d) indicates the ϕ above which local orientational correlations are scale-free.

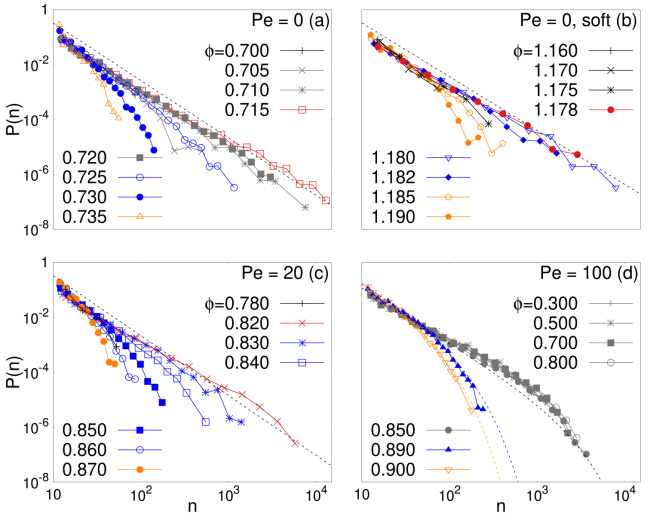

FIG. 3. (Color online.) Cluster size distribution for (a) passive hard-disks, (b) soft-disks, (c) ABP at Pe = 20 and (d) Pe = 100 at different ϕ. We represent in red the curve we identify with percolation-like behavior. We show an algebraic decay $P(n) \propto n^{-\tau}$ with $\tau = 2.09$, 2.08 and 2.18 for (a), (b) and (c), respectively, $\tau = 1 + d/d_f$. In (d) the dashed lines are $n^{-2}e^{-n/n^*}$ decays with $n^* = 30$, 10^2 and 2.10^3 in the solid, hexatic and MIPS.

To clarify whether grain boundaries or defect clusters show percolation-like behaviour and, if so, its connection with 2D melting [12, 18, 19, 33–35], we use the framework of percolation theory [36]. Grain boundaries are visually identifiable as chains of closely spaced defects (see Fig. 1), though the latter are not fully connected at the single cell scale. The microscopic gaps are filled via a coarse-graining procedure, routinely applied to study gelation [37]. To be quantitative, we divide our system into cells of linear size d_s [38], and define a coarse-grained cluster as a set of connected cells with, at least, one defect. In the following we use $d_s = 3\sigma_d$ (see SM [31] for a discussion) and analyze the cluster size distribution $P(n)$ obtained by measuring the number of coarse-grained clusters made of n defected cells, excluding the spanning one.

In Fig. 3 we show $P(n)$ for (a) passive hard-disks, (b) soft-disks, (c) ABP at Pe = 20 and (d) Pe = 100, and varying ϕ across the different phase transitions. Starting from the solid, the effect of decreasing ϕ is clear for all Pe, as the distribution broadens to include larger clusters. For passive disks, both hard and soft, and at Pe = 20, $P(n)$ becomes scale free (very) close to the value

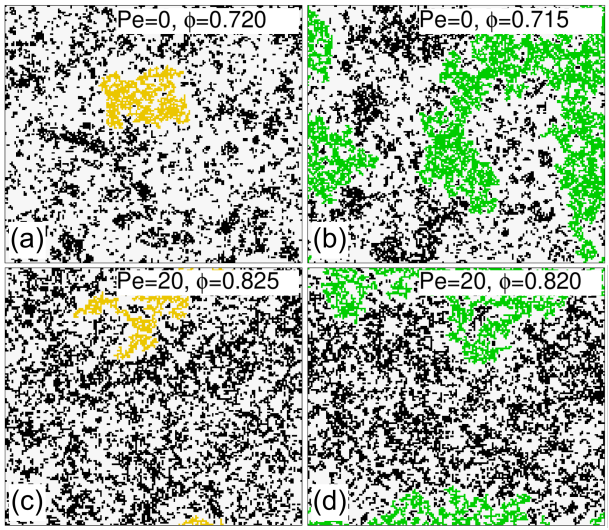

FIG. 4. (Color online.) Coarse-grained clusters of defects. The largest cluster is painted yellow or green whether it percolates or not. Pe = 0 in (a) $\phi = 0.720$ and (b) $\phi = 0.715$. Pe = 20 in (c) $\phi = 0.825$ and (d) $\phi = 0.820$.

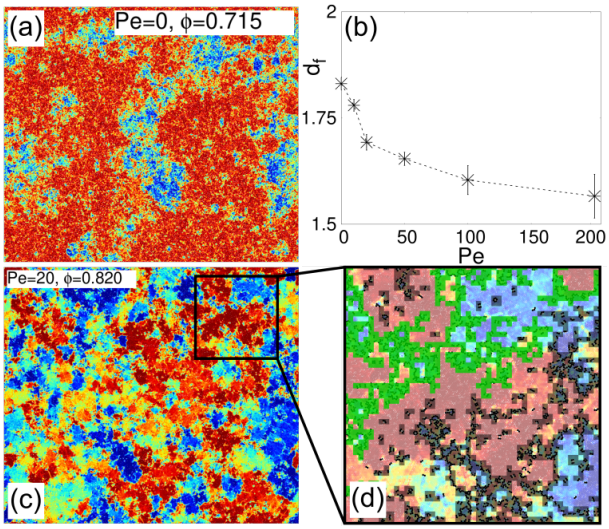

FIG. 5. (Color online.) Map of $\psi_6(\mathbf{r})$, projected on the mean orientation, for equilibrium hard-disks (a) and active hard-disks (c). (b) Fractal dimension as a function of Pe at the hexatic-liquid transition. (d) Zoom over the square in (c) with the defect cluster shown in green over the $\psi_6(\mathbf{r})$ background.

of ϕ above which orientational correlations become algebraic. In Fig. 3 we show $P(n) \sim n^{-\tau}$, with τ fixed from $\tau = 1 + d/d_{\rm f}$, $d_{\rm f}$ being the fractal dimension of the clusters (see below). In the finite systems studied, at the hexatic-liquid transition, the statistics of the coarse-grained clusters is close to the one of clusters at critical percolation, irrespective of its discontinuous (for passive hard-disks [17]) or continuous (for passive soft disks [18] and ABP at Pe = 20 [26]) character. At Pe = 100, MIPS preempts the liquid-hexatic transition and thus the percolation-like behavior. The size distribution remains largely invariant within MIPS at fixed Pe, similarly to what we saw in Fig. 2 (d).

The percolation of coarse-grained clusters is further evidenced by the snapshots shown in Fig. 4. For equilibrium hard-disks in the solid phase, the largest cluster (in yellow) does not span the system. As we decrease ϕ, the size distribution broadens until a percolating cluster arises (in green), right in the middle of the liquid-hexatic coexistence region [26]. The location of the percolating structure is correlated with the one of the liquid. This is shown by the map of the local hexatic order parameter, $\psi_6(\mathbf{r}_j) = N_j^{-1} \sum_{k \in \partial_j} e^{i6\theta_{jk}}$, where θ_{jk} is the angle formed by the segment that connects the center of the jth disk and the one of its kth, out of N_j nearest neighbors, see Fig. 5 (a). (They are also the regions of low local density [26].) Indeed, most defects are in the liquid-hexatic boundaries, *cfr.* Fig. 4 (b) and Fig. 5 (a), and the emergence of a percolating cluster at Pe = 0 can be attributed to the percolation of the liquid domain. For Pe = 20, there is no liquid-hexatic coexistence, and yet there is percolation close to the hexatic-liquid transition (also for soft particles, not shown here, see [31]). In this case, coarse-grained clusters can be identified with grain-boundaries, as shown in Fig. 5 (c)-(d), and percolation with the emergence of a system-spanning network of them. Finally, at higher Pe, in the MIPS regime, we see large hexatic domains, leaving behind a network of grain-boundaries, that can become large but remains finite, see [31].

An essential aspect of critical percolation is the fractal morphology of the clusters. A way to study their geometry is to relate their size, $n_{\mathcal{C}}$, to a length scale, *e.g.*, their radius of gyration $R_{g_{\mathcal{C}}} = [\sum_{i \in \mathcal{C}} (\mathbf{r}_i - \mathbf{r}_{\mathcal{C}})^2 / n_{\mathcal{C}}]^{\frac{1}{2}}$ (the sum runs over all cells in the cluster and $\mathbf{r}_{\mathcal{C}}$ is the position of its center of mass) *via* the fractal dimension $d_{\rm f}$: $n_{\mathcal{C}} \sim {R_{g_{\mathcal{C}}}}^{d_{\rm f}}$. At criticality, the hyper-scaling relation $\tau = d/d_{\rm f} + 1$ (d being the space dimensionality) relates $d_{\rm f}$ to the exponent τ of the size distribution. The evolution of $d_{\rm f}$ with Pe, is shown in Fig. 5 (b), suggesting that clusters get more ramified as Pe increases, in agreement with Fig. 4. Indeed, for higher Pe, local crystalline order is enhanced leaving behind sharper grain boundaries and thus string-like clusters with smaller $d_{\rm f}$. The measurement of $d_{\rm f}$ provides a consistent prediction for τ in $P(n)$, as shown in Fig. 3.

Experience teaches us that we have to be extremely careful before claiming that there is a strict relation between a thermodynamic phase transition driven by the competition between interactions and fluctuations, such as melting, and a phenomenon of purely geometric nature, like percolation. In many spin models, the properties of their second order thermal phase transitions can be rigorously described in terms of the critical percolation of suitably defined Fortuin-Kasteleyn (FK) clusters,

that *are not* the obvious geometric ones one could *a priori* try to use [36, 39]. Although the FK clusters should not be useful to describe a first order thermodynamic transition, in cases with very long correlation lengths such as the 2D Potts model with $Q \gtrsim 4$, one could easily see them percolate close to the transition in finite size samples [40]. Our simulation results (on finite systems) provide clear evidencies that active, passive, continuous and discontinuous hexatic-liquid transitions are accompanied by the percolation of defect clusters. However, we cannot posit that the relevant clusters to describe the transition are the (coarse-grained) defect ones we used and, therefore, we cannot establish a rigorous connexion between melting and percolation.

We have characterized the melting of passive and active disks in terms of the statistics of topological defects. On the one hand, we found that a KTHNY scenario describes the transition from the solid to the hexatic for all values of the activity. Next, we generically observed the percolation of clusters of defects at the vicinity of the hexatic-liquid transition. Although such a percolation has been usually associated to first-order melting scenarios, we found it across both first and second-order transitions, in- and out-of-equilibrium. The geometry of the percolating cluster depends, though, on the activity. While we see percolation of a liquid phase across the first order transition in equilibrium hard disks, the clusters that percolate across the melting of the active hexatic, at intermediate Pe, are due to grain boundaries. At high Pe, MIPS prevails over the hexatic-liquid transition, and clusters of defects are large and ramified, but do not percolate. The present work clarifies the nature of phase transitions in systems of active particles and sheds new light on the old problem of 2D melting.

Acknowledgments. We thank M. Picco for very useful discussions. We acknowledge access to the MareNostrum Supercomputer at the BSC, IBM Nextscale GALILEO at CINECA (Project INF16-fieldturb) under CINECA-INFN agreement and Bari ReCaS e-Infrastructure funded by MIUR *via* PON Research and Competitiveness 2007-2013 Call 254 Action I.

[1] N. D. Mermin and H. Wagner, Phys. Rev. Lett. **17**, 1133 (1966).
[2] N. D. Mermin, Phys. Rev. **176**, 250 (1968).
[3] V. Berezinskii, Sov. Phys. JETP **32**, 493 (1971).
[4] J. M. Kosterlitz and D. J. Thouless, J. Phys. C: Solid State Physics **6**, 1181 (1973).
[5] K. J. Strandburg, Rev. Mod. Phys. **60**, 161 (1988).
[6] M. A. Glaser and N. A. Clark, Adv. Chem. Phys. **83**, 543 (1992).
[7] B. I. Halperin and D. R. Nelson, Phys. Rev. Lett. **41**, 121 (1978).
[8] A. Young, Phys. Rev. B **19**, 1855 (1979).
[9] K. Zahn, R. Lenke, and G. Maret, Phys. Rev. Lett. **82**, 2721 (1999).
[10] K. Chen, T. Kaplan, and M. Mostoller, Phys. Rev. Lett. **74**, 4019 (1995).
[11] S. Prestipino, F. Saija, and P. V. Giaquinta, Phys. Rev. E **71**, 050102 (2005).
[12] W.-K. Qi, Z. Wang, Y. Han, and Y. Chen, J. Chem. Phys. **133**, 234508 (2010).
[13] K. Wierschem and E. Manousakis, Phys. Rev. B **83**, 214108 (2011).
[14] S. Chui, Phys. Rev. Lett. **48**, 933 (1982).
[15] S. Chui, Phys. Rev. B **28**, 178 (1983).
[16] H. Kleinert, Physics Letters A **95**, 381 (1983).
[17] E. P. Bernard and W. Krauth, Phys. Rev. Lett. **107**, 155704 (2011).
[18] S. C. Kapfer and W. Krauth, Phys. Rev. Lett. **114**, 035702 (2015).
[19] W. Qi, A. P. Gantapara, and M. Dijkstra, Soft Matter **10**, 5449 (2014).
[20] A. L. Thorneywork, J. L. Abbott, D. G. A. L. Aarts, and R. P. A. Dullens, Phys. Rev. Lett. **118**, 158001 (2017).
[21] M. E. Cates, Rep. Prog. Phys. **75**, 042601 (2012).
[22] M. C. Marchetti, J.-F. Joanny, S. Ramaswamy, T. B. Liverpool, J. Prost, M. Rao, and R. A. Simha, Rev. Mod. Phys. **85**, 1143 (2013).
[23] M. R. Shaebani, A. Wysocki, R. G. Winkler, G. Gompper, and H. Rieger, arXiv preprint arXiv:1910.02528 (2019).
[24] J. Bialké, T. Speck, and H. Löwen, Phys. Rev. Lett. **108**, 168301 (2012).
[25] C. A. Weber, C. Bock, and E. Frey, Phys. Rev. Lett. **112**, 168301 (2014).
[26] P. Digregorio, D. Levis, A. Suma, L. F. Cugliandolo, G. Gonnella, and I. Pagonabarraga, Phys. Rev. Lett. **121**, 098003 (2018).
[27] J. U. Klamser, S. C. Kapfer, and W. Krauth, Nat. Comm. **9**, 5045 (2018).
[28] S. Paliwal and M. Dijkstra, arXiv:1907.04767 (2019).
[29] M. E. Cates and J. Tailleur, Annu. Rev. Cond. Matt. Phys. **6**, 219 (2015).
[30] D. Levis, J. Codina, and I. Pagonabarraga, Soft Matter **13**, 8113 (2017).
[31] See Supplementary Material at doi:.
[32] A. Pertsinidis and X. Ling, Phys. Rev. Lett. **87**, 098303 (2001).
[33] F. L. Somer Jr, G. Canright, T. Kaplan, K. Chen, and M. Mostoller, Phys. Rev. Lett. **79**, 3431 (1997).
[34] F. L. Somer Jr, G. Canright, and T. Kaplan, Phys. Rev. E **58**, 5748 (1998).
[35] S. Deutschländer, C. Boitard, G. Maret, and P. Keim, Phys. Rev. E **92**, 060302 (2015).
[36] D. Stauffer and A. Aharony, *Introduction to percolation theory* (Taylor & Francis, 2018).
[37] A. Coniglio, L. De Arcangelis, E. Del Gado, A. Fierro, and N. Sator, J. Phys.: Cond. Matt. **16**, S4831 (2004).
[38] These are $d_x \times d_y$ cells, where $d_{x,y} = L_{x,y}/\mathrm{int}(L_{x,y}/ds)$.
[39] C. M. Fortuin and P. W. Kasteleyn, Physica **57**, 536 (1972).
[40] M. Picco, (2019), private communication.